ELSEVIER

Thermochimica Acta 374 (2001) 73–83

thermochimica acta

www.elsevier.com/locate/tca

Kinetic analysis on the crystallization of some alloys from the Sb–As–Se glassy system

P.L. López-Alemany, J. Vázquez*, P. Villares, R. Jiménez-Garay

Departamento de Física de la Materia Condensada, Facultad de Ciencias, Universidad de Cádiz, Apartado 40, 11510 Puerto Real (Cádiz), Spain

Received 29 May 2000; received in revised form 7 December 2000; accepted 28 February 2001

Abstract

An alternative method is proposed for generalizing the Johnson–Mehl–Avrami equation, under restrictive assumptions for non-isothermal transformations on the basis of nucleation and crystal growth processes. An interesting result, according to literature, is that the Kissinger equation can be applied to the analysis of heterogeneous solid state transformations. Bearing in mind the quoted generalization, the isothermal and non-isothermal crystallization kinetics of $Sb_{0.16}As_zSe_{0.84-z}$ ($z = 0.22$, 0.29, 0.36, 0.43) glassy alloys have been analyzed using differential scanning calorimetric (DSC) data. The kinetic parameters calculated from both sets of calorimetric data are in agreement, within experimental error, with the use of adequate equations and assumptions clearly stated for each regime. The obtained results indicate that the crystallization of these alloys is a thermally activated process and it is mainly controlled by a volume nucleation mechanism. The $z = 0.43$ alloy shows the strongest stability against crystallization, while the $z = 0.36$ alloy is the least stable composition among analyzed alloys. The phases that crystallize with the thermal treatment have been identified by X-ray diffraction. The diffractograms of the transformed materials suggest the presence of microcrystallites of Sb_2Se_3 and AsSe, embedded in a residual amorphous matrix.

Keywords: Glassy alloy; Transformation kinetics; Isothermal and non-isothermal processes; Heating rate; Kinetic parameters; Thermal stability; Crystalline phases

1. Introduction

Amorphous materials themselves are nothing new. Man has been making glasses (mainly silica) for centuries, however, it has been only in recent years that ''glass science'' has emerged as a field of study in its own right. The last decades have seen a strong theoretical and practical interest in the application of isothermal and non-isothermal experimental analysis techniques to the study of glass–crystal transformations. While isothermal experimental analysis techniques are in most cases more definitive, non-isothermal thermoanalytical techniques have several advantages. These techniques can be used to extend the temperature range of measurements beyond that accessible to isothermal experiments. Many phase transformations occur too rapidly to be measured under isothermal conditions because of transients inherently associated with the experimental apparatus. Industrial processes often depend on the kinetic behavior of systems undergoing phase transformation under non-isothermal conditions. In this instance, a

* Corresponding author. Tel.: +349-56-830966; fax: +349-56-016288.
E-mail address: jose.vazquez@uca.es (J. Vázquez).

0040-6031/01/$ – see front matter
PII: S0040-6031(01)00490-7

reliable measurement of non-isothermal transformation kinetics is desirable.

The study of crystallization kinetics in glass-forming liquids has often been limited by the elaborate nature of the experimental procedures that are employed. The increasing use of thermoanalytical techniques such as differential thermal analysis (DTA) or differential scanning calorimetry (DSC) has, however, offered the promise of obtaining useful data with simple methods. A popular thermal analysis method developed by Kissinger [1,2] determines the kinetic parameters from graphs of the logarithm of the quotient T_p^2/β (β is the heating rate) versus the reciprocal of the temperature, T_p, at the maximum of the reaction rate in non-isothermal experiments. This method was frequently used in studies of the crystallization of glassy alloys [3–6] despite the fact that literature [7] on thermal analysis techniques reflected a consensus that application of the Kissinger method to solid state reactions is improper. However, the notable work of Henderson [8] has provided a theoretical basis for the treatment of non-isothermal analysis techniques and justifies the use of the Kissinger method for many solid state transformations.

In this work, an alternative method is proposed for analyzing the non-isothermal (constant heating rate) crystallization kinetics on the basis of nucleation and crystal growth processes. Surprising results of this analysis, in agreement with that provided by Henderson [8], are that in the constant heating rate case, the descriptive function, $\ln(T_p^2/\beta) = f(T_p^{-1})$, is essentially independent of the reaction order, this is, of the kinetic exponent, n, and that the Kissinger equation holds. Thus, although the basic equation in Kissinger's analysis of homogeneous (first-order) transformations is indeed inappropriate for heterogeneous (higher-order) solid state transformations, the Kissinger method can be applied to the analysis of heterogeneous transformations. In addition, the present method is applied to the isothermal and non-isothermal DSC data for the analysis of the crystallization kinetics of glassy alloys $Sb_{0.16}As_zSe_{0.84-z}$ with $z = 0.22$, 0.29, 0.36 and 0.43. From this analysis it is observed that the proposed method to study non-isothermal data is accurate and reliable. Finally, the crystalline phases corresponding to the crystallization products were identified by X-ray diffraction (XRD) measurements, using Cu Kα radiation.

2. Theoretical basis of the calorimetric measurements

In the DSC, the instrument supplies heat to either the sample being investigated or the reference material in order to keep their temperatures equal. The instantaneous differential heat supplied to the sample and reference is available as the output signal. The fraction of material transformed at any time is proportional to the amount of heat evolved only when the crystalline product of the reaction has the same chemical composition than the glass (polymorphous transformation) or even when the crystalline mixture that precipitates has a mean composition identical to the precursor glass (eutectic transformation). However, the proportionality becomes an approximation when the mean chemical composition of the crystalline phases differs from the global one, because so does that of the remaining amorphous phase. Then, the area of the exothermic crystallization DSC peak is equal to the difference between the enthalpy of the initial disordered solution phase and that of the mixture of crystalline product plus the transformed remaining disordered solution phase.

3. Theoretical basis of the model

The extraction of the reaction rate, dx/dt, at any time from a DSC measurement is not straightforward because the assumption of proportionality between dx/dt and the heat flow is very restrictive. It only holds for polymorfic transformation. Even if in the average a transformation produces an eutectic mixture, it may be the result of an initial precipitation of a primary phase which activates the eutectic transformation of the remaining disordered solution phase.

Bearing in mind the above restriction, the DSC output, Q_{DSC}, is assumed to be proportional to the reaction rate, dx/dt ($Q_{DSC} = C\,dx/dt$, C is a constant) so the volume fraction crystallized, $x(t)$, is given by $x(t) = A(t)/A$, were

$$A(t) = \int_0^t Q_{DSC}\,dt' = C[x(t) - x(0)]$$

and $A = A(\infty)$.

3.1. Isothermal regime

The theoretical basis for interpreting kinetic data ($x(t)$ or dx/dt) is provided by the formal theory of transformation kinetics [9–13]. This theory describes the evolution with time, t, of the volume fraction crystallized, x, by

$$x(t) = 1 - \exp[-(Kt)^n] \tag{1}$$

provided nuclei either form at a constant nucleation rate or they pre-exist, and grow at a constant rate.

In Eq. (1), K is defined as the effective overall reaction rate constant, whose temperature dependence is usually expressed in a limited temperature range by the Arrhenius equation

$$K = K_0 \exp\left(-\frac{E}{RT}\right) \tag{2}$$

where K_0 is the frequency factor, T the absolute temperature, and E the effective activation energy describing the overall crystallization process.

Once the two basic assumptions to use Eqs. (1) and (2) have been clearly stated under isothermal regime, it should be noted that Eq. (1) describes isothermal processes so $K(T)$ is a constant, which depends on the temperature. An expression for the reaction rate, dx/dt, can be derived by differentiating the Eq. (1) with respect to t, at constant temperature, giving

$$\frac{dx}{dt} = nK^n t^{n-1}(1-x) = nK(1-x)[-\ln(1-x)]^{(n-1)/n} \tag{3}$$

which is a simple function of the temperature and the volume fraction transformed. However, the results can be more correctly analyzed by Eq. (1). Taking twice the logarithm of Eq. (1) leads to the expression

$$\ln[-\ln(1-x)] = n\ln K + n\ln t. \tag{4}$$

At a given temperature, values of n and K are determined from $x(t)$ data using Eq. (4) by least-squares fitting of $\ln[-\ln(1-x)]$ versus $\ln t$. Values of the $\ln K$ are evaluated at different temperatures by repeating the same procedure. The activation energy and frequency factor are then evaluated from the logarithmic form of Eq. (2) by least-squares fitting $\ln K$ versus $1/T$.

3.2. Non-isothermal regime

In a non-isothermal DSC experiment, the sample temperature changes linearly with time, t, at a constant heating rate $\beta(= dT/dt)$, namely

$$T = T_0 + \beta t \tag{5}$$

where T_0 is the initial temperature. In the case of non-isothermal regime, the rate constant K, changes continually with time due to the change of the temperature and Eq. (1) becomes

$$x(t) = 1 - \exp\left[-\left(\int_0^t K[T(t')]\,dt'\right)^n\right] = 1 - \exp(-I^n) \tag{6}$$

where $K[T(t')]$ is still given by Eq. (2) and $T(t')$ is the temperature at t'. Note that the volume fraction crystallized depends on t through the temperature history $T(t)$ and the same is true for the integral I.

Deriving with respect to time in Eq. (6), the crystallization rate is obtained as

$$\frac{dx}{dt} = nK(1-x)I^{n-1}. \tag{7}$$

The maximum crystallization rate is found by making $d^2x/dt^2 = 0$, thus obtaining the relationship

$$nK_p(I^n)|_p = \beta\frac{EI_p}{RT_p^2} + (n-1)K_p \tag{8}$$

where the quantity values, which correspond to the maximum crystallization rate, are denoted by subscript 'p'.

On the other hand, the time integral in Eq. (6) is transformed to a temperature integral, yielding

$$I(T) = \frac{K_0}{\beta}\int_{T_0}^{T} \exp\left(-\frac{E}{RT'}\right)dT' \tag{9}$$

which is not integrable in closed form and is represented in [14–17] by several approximate analytical expressions. In this work, by using the substitution $y' = E/RT'$, the above integral has been represented, according to [17], by the sum of the alternating series

$$S(y') = -\frac{e^{-y'}}{y'^2}\sum_{k=0}^{\infty}\frac{(-1)^k(k+1)!}{y'^k}.$$

Considering that in this type of series the error produced is less than the first term neglected and bearing

in mind that in most crystallization reactions $y' = E/RT' \gg 1$ (usually $E/RT' \geq 25$), it is possible to use only the two first terms of this series and the error introduced is not greater than 1%. In addition, if it is assumed that $T^2(1 - 2RT/E)\exp(-E/RT) \gg T_0^2(1 - 2RT_0/E)\exp(-E/RT_0)$, Eq. (9) becomes

$$I = K_0 E(\beta R)^{-1} e^{-y} y^{-2}(1 - 2y^{-1}) = RT^2 K(\beta E)^{-1}(1 - 2RTE^{-1}). \quad (10)$$

Substituting the last expression of I in Eq. (8), one obtains

$$I_p = \left(1 - \frac{2RT_p}{nE}\right)^{1/n}$$

relationship that when it is equated to the Eq. (10) gives

$$RT_p^2(\beta E)^{-1} K_0 \exp\left(-\frac{E}{RT_p}\right) = \left(1 - \frac{2RT_p}{nE}\right)^{1/n}\left(1 - \frac{2RT_p}{E}\right)^{-1} \quad (11)$$

or in a logarithmic form

$$\ln\left(\frac{T_p^2}{\beta}\right) + \frac{\ln K_0 R}{E} - \frac{E}{RT_p} \approx \left(\frac{2RT_p}{E}\right)\left(1 - \frac{1}{n^2}\right) \quad (12)$$

where the function $\ln(1 - z)$ with $z = 2RT_p/nE$ or $z = 2RT_p/E$ is expanded as a series and only the first term has been taken.

Note that Eq. (12) reduces to the Kissinger expression for the $n = 1$ case as one might have anticipated since this corresponds to the homogeneous reaction case. Moreover, for most crystallization reactions the right-hand side (RHS) of Eq. (12) is generally negligible in comparison to the individual terms on the left hand side for common heating rates ($\leq$100 K min^{-1}). Thus, it can be seen that the Kissinger method is appropriate for the analysis not only of homogeneous reactions, but also for the analysis of heterogeneous reactions which are described by the JMA equation in isothermal experiments. The approximation in Eq. (12) (RHS = 0), implies

$$\frac{d\left[\ln(T_p^2/\beta)\right]}{d(1/T_p)} = \frac{E}{R},$$

where the quoted approximation might introduce a 3% error in the value of E/R in the worst cases (typically, $n > 1$ and $E/RT_p > 25$ which suggests that the error introduced in E/R by setting the RHS of Eq. (12) = 0 is considerably less than 1%). Eq. (12) also serves to determine the frequency factor, K_0, from the intercept of a $\ln(T_p^2/\beta)$ versus $1/T_p$ plot. Eq. (7), which describes the time dependence of the reaction rate, and Eq. (12), which allows for the simple extraction of the parameters K_0 and E by means of the Kissinger method, form the basis for the analysis of constant heating rate data.

Finally, according to [6,18], the kinetic exponent, n, can be evaluated from Eqs. (6) and (10). In this sense, considering the same assumptions used to get Eq. (10) and taking the logarithm of the quoted equation leads to an expression that, in the range of values of $y = E/RT$, $25 \leq y \leq 55$, can be fitted very satisfactorily by a linear approximation (an additional assumption), yielding

$$\ln\left[e^{-y} y^{-2}(1 - 2y^{-1})\right] \cong -5.304 - 1.052y$$

and Eq. (10) becomes

$$I = K_0 E(\beta R)^{-1} \exp(-5.304 - 1.052y) \quad (13)$$

where the above-mentioned approximation might introduce a 5.8% error in the value of $(e^{-y} y^{-2}(1 - 2y^{-1}))$ in the worst cases. Substituting Eq. (13) into logarithmic form of Eq. (6), one obtains

$$-\ln(1 - x) = C_0 \beta^{-n} \exp\left(-\frac{1.052nE}{RT}\right) \quad (14)$$

where $n = m$, the dimensionality of the crystal growth in the case of "site saturation" (pre-existing nuclei). Vázquez et al. [6], by using the same assumptions, have generalized the above equation by means of the relationship

$$-\ln(1 - x) = C_0 \beta^{-n} \exp\left(-\frac{1.052mE}{RT}\right) \quad (15)$$

with $n = m + 1$ for a quenched glass containing no nuclei and $n = m$ for a glass containing a sufficiently large number of nuclei. Taking the logarithm of Eq. (15) leads to the expression

$$\ln[-\ln(1 - x)] = -n \ln \beta - \frac{1.052mE}{RT} + \ln C_0 \quad (16)$$

which, for constant temperature, represents a straight line whose slope is $-n$, i.e.

$$\frac{d\{\ln[-\ln(1-x)]\}}{d(\ln\beta)} = -n \quad (17)$$

Thus, using a multiple scan analysis technique: first, volume fraction, x, at the same temperature from a number of crystallization exotherms under different heating rates is calculated by the ratio of partial area to the total area of crystallization exotherm. After plotting $\ln[-\ln(1-x)]$ versus $\ln\beta$, and if the data can be fitted to the linear function, then the slope of the quoted function is the kinetic exponent.

4. Experimental details

The semiconducting alloys $Sb_{0.16}As_zSe_{0.84-z}$ with $z = 0.22$, 0.29, 0.36 and 0.43 were made in bulk form, from their components of 99.999% purity, which were pulverized to particles of size less than 64 μm, mixed in adequate proportions, and introduced into quartz ampoules. The capsules were subjected to an alternating process of filling and vacuuming of inert gas in order to ensure the absence of oxygen inside. This ended with a final vacuuming process of up to 10^{-2} N m^{-2}, and sealing with an oxyacetylene burner. The ampoules were put into a furnace at around 1225 K for 24 h, turning at 1/3 rpm, in order to ensure the homogeneity of the molten material, and then quenched in water to avoid crystallization. The capsules containing the samples were then put into a mixture of hydrofluoric acid and hydrogen peroxide in order to corrode the quartz and make it easier to extract the alloys. The glassy nature of the quoted alloys was confirmed by diffractometric X-ray scan, in a Siemens D500 diffractometer, showing an absence of the peaks which are characteristic of crystalline phases. The homogeneity and composition of the samples were verified through SEM in a Jeol, scanning microscope JSM-820. The thermal behavior of the materials was investigated using a Perkin-Elmer DSC7 differential scanning calorimeter with an accuracy of ±0.1 K. Temperature and energy calibrations of the instrument were performed using the well-known melting temperatures and melting enthalpies of high purity zinc and indium supplied with the instrument. Powdered samples weighing about 20 mg (particles size around 40 μm) were crimped in aluminum pans, an empty aluminum pan was used as reference. A constant flow of nitrogen was maintained in order to provide a constant thermal blanket within the DSC cell, thus eliminating thermal gradients, and ensuring the validity of the applied calibration standard from sample to sample. Moreover, the nitrogen purge allows to expel the gases emitted by the reaction, which are highly corrosive to the sensory equipment installed in the DSC furnace.

The technique for extracting the kinetic exponent n and $K(T)$ in an isothermal experiment was previously described. Non-isothermal transformation kinetic data for the above-mentioned alloys were obtained by scanning of the samples from the room temperature through their glass transition temperature, T_g, at different heating rates between 2 and 64 K min^{-1}.

Finally, with the aim of investigating the phases into which the samples crystallize, diffractograms of the alloys transformed after the thermal treatments were obtained. The experiments were performed with a Philips diffractometer (type PW 1830). The patterns were run with Cu as target and Ni as filter ($\lambda = 1.542$ Å) at 40 kV and 40 mA, with a scanning speed of 0.1° s^{-1}.

5. Results

5.1. Isothermal crystallization of $Sb_{0.16}As_zSe_{0.84-z}$ glasses

Isothermal DSC measurements were performed at various temperatures for samples of four glass compositions of $z = 0.22$, 0.29, 0.36 and 0.43, the evolution of their DSC exotherms for crystallization were recorded. Since each glass composition has a different glass transition temperature, T_g (listed in Table 1), the isothermal crystallization temperature, T_{iso} (see Table 1) was chosen in a $(T_{iso} - T_g)$ interval, whose mean value is (65–85 K), so that the thermal stability of the different alloys could be relatively compared. Fig. 1 shows the isothermal DSC traces at temperatures of 468, 473, 478, 483, 488 K for $z = 0.22$ sample. It should be noted that the quantity t_i is the lapsed time since the constant temperature of the isothermal process is reached, until the crystallization peak begins, this is, when the transformed fraction is

Table 1
The value of n, K, K_0, and $-\Delta H$ of $Sb_{0.16}As_zSe_{0.84-z}$ alloys in isothermal crystallization

z	T_g (K)	T_{iso} (K)	n	$K \times 10^4$ (s^{-1})	K_0 (s^{-1})	E (kJ mol^{-1})	$-\Delta H$ (J g^{-1})
0.22	401	468	2.4 ± 0.4	9.1 ± 0.6	1.3×10^{10}	111 ± 3	37 ± 2
		473	2.6 ± 0.2	11.5 ± 1.0			34 ± 1
		478	2.3 ± 0.4	15.8 ± 1.0			37 ± 1
		483	2.3 ± 0.2	21.4 ± 2.1			31 ± 1
		488	2.3 ± 0.2	30.6 ± 3.5			30 ± 1
0.29	441	503	2.4 ± 0.5	13.9 ± 1.0	4.7×10^{14}	171 ± 5	35 ± 2
		508	2.3 ± 0.4	19.4 ± 1.8			35 ± 1
		513	2.4 ± 0.2	21.6 ± 2.1			36 ± 1
		518	2.3 ± 0.4	38.8 ± 4.2			42 ± 1
		523	2.3 ± 0.2	70.3 ± 4.8			45 ± 2
0.36	486	543	2.4 ± 0.5	15.2 ± 1.0	1.6×10^{14}	178 ± 5	28 ± 2
		548	2.4 ± 0.4	17.8 ± 1.5			30 ± 2
		553	2.3 ± 0.2	25.3 ± 1.6			28 ± 2
		558	2.2 ± 0.4	37.4 ± 3.7			33 ± 3
		563	2.1 ± 0.2	60.3 ± 4.1			35 ± 3
0.43	481	553	2.5 ± 0.5	13.3 ± 1.0	4.6×10^{11}	152 ± 4	14 ± 1
		558	2.4 ± 0.2	17.3 ± 1.5			16 ± 1
		563	2.2 ± 0.5	22.1 ± 2.3			18 ± 1
		568	2.1 ± 0.2	32.6 ± 3.5			20 ± 2
		573	2.0 ± 0.2	45.3 ± 4.5			27 ± 2

approximately 1%. In addition, it is well known that with an increase of T_{iso}, the time for the completion of crystallization diminishes, and the height of DSC exotherms increases. This experimental result indicates that the crystallization of $Sb_{0.16}As_zSe_{0.84-z}$ alloys is a thermally activated process, i.e. some activation energy is required to trigger its occurrence. In the DSC measurements, isothermal crystallization time and heat flow were automatically recorded. Computer programs were employed to calculate volume fraction transformed, x, at different time, t. The x–t curves for $z = 0.22$ composition at different

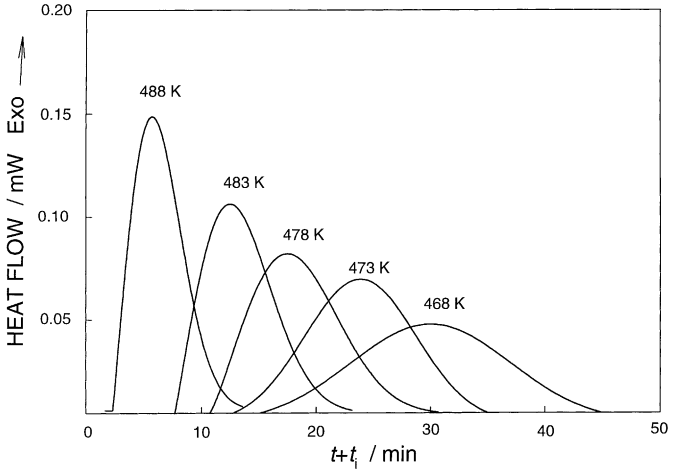

Fig. 1. DSC curves of isothermal crystallization for $z = 0.22$ glass.

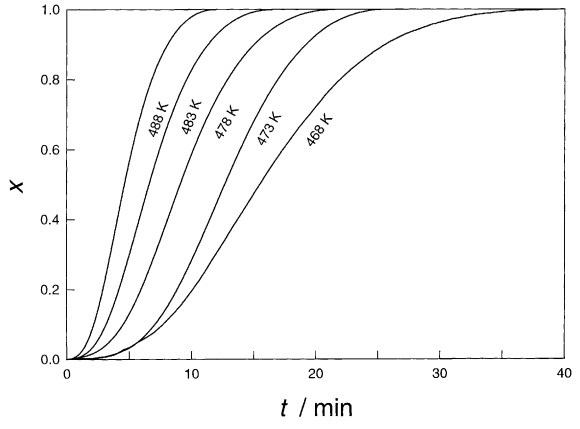

Fig. 2. The x–t curves of isothermal crystallization for $z = 0.22$ glass.

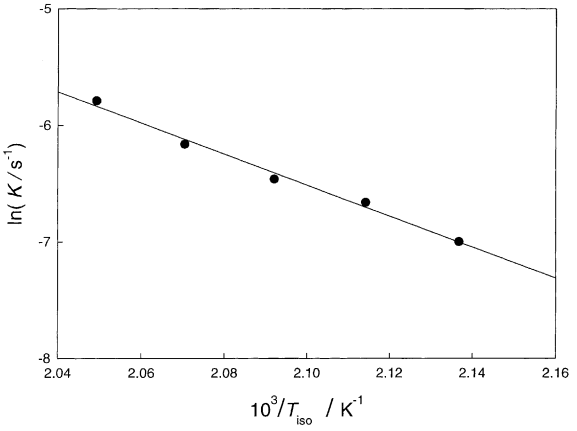

Fig. 4. Arrhenius plots of isothermal crystallization for $z = 0.22$ glass.

isothermal crystallization temperatures are shown in Fig. 2. It can be observed from these curves that at higher T_{iso}, x changes more rapidly with t, the crystallization process proceeds more quickly than at lower T_{iso}. The $\ln[-\ln(1-x)] - \ln t$ curves of the same glass sample are presented in Fig. 3. The data of $\ln[-\ln(1-x)]$ and $\ln t$ are fitted to linear functions by least squares fitting. From the slope and intercept of these fits, kinetic exponent, n, and reaction rate constant, K, could be determined. From the slope and intercept of the straight line in Fig. 4 where the Arrhenius relationship for $z = 0.22$ glass is illustrated, activation energy, E, and frequency factor, K_0, can be estimated through least-squares fits of $\ln K$ versus $10^3/T_{iso}$. The kinetic parameters such as n, K, K_0, E and $-\Delta H$ for all glass compositions under isothermal conditions are listed in Table 1. These parameters are obtained according to the above procedure through linear least-squares fitting of experimental data, and are justified by the correlation factors ≥ 0.983. In Fig. 5 ($T_{iso} - T_g$) is plotted against t as time–temperature–transformation (T–T–T) graphs. It is well known that several T–T–T diagrams may be constructed, and each one is characterized by a specific fixed value of the transformed fraction, x. Therefore, it should be noted that in the present paper the annealing temperature is plotted versus time, t, at which ends the crystallization peak, this is $x \approx 1.0$. The above mentioned figure

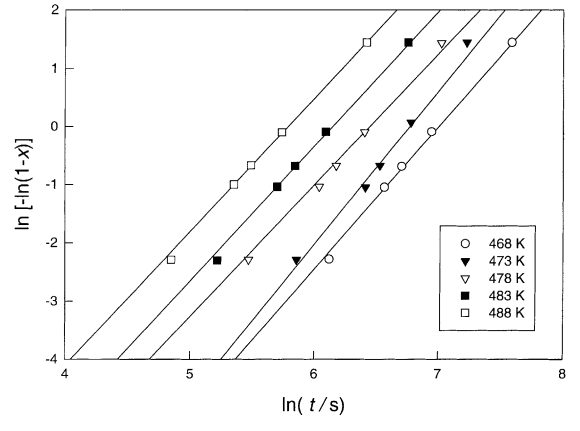

Fig. 3. Plots for extracting the kinetic exponent, n, in Eq. (1) (as described in the text).

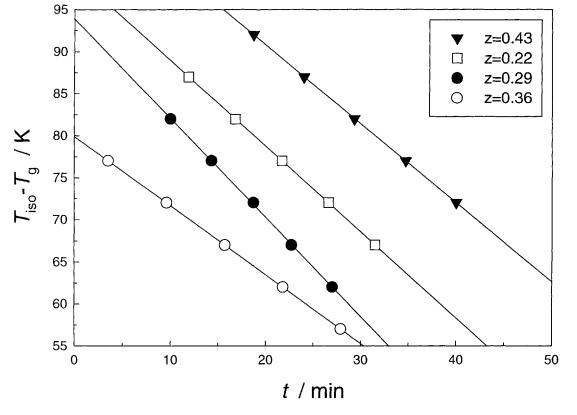

Fig. 5. The T–T–T graph of different alloys of the $Sb_{0.16}As_z$ $Se_{0.84-z}$ glassy system.

reveals the difference of glass stability among $Sb_{0.16}As_zSe_{0.84-z}$ compositions. For example, at a given $(T_{iso} - T_g) = 77$ K, it takes approximately 10 times as long to fully crystallize a $z = 0.43$ sample as it does to crystallize the same fraction, this is $x \cong 1.0$, of $z = 0.36$ sample.

5.2. Non-isothermal crystallization of $Sb_{0.16}As_zSe_{0.84-z}$ glasses

DSC measurements of glass samples were carried out at various heating rates ($\beta = 1$, 2, 4, 8, 16, 32 and 64 K min^{-1}, respectively). The typical DSC exotherms of $z = 0.22$ glass are exhibited in Fig. 6. It is seen that the peak temperature, T_p, shifts to higher temperature with increasing heating rate, in the meantime, the peak height increases and the area under the

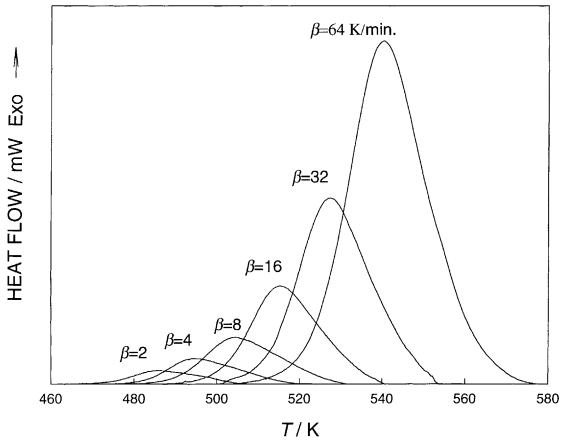

Fig. 6. DSC traces of $z = 0.22$ glass at different heating rates.

Table 2
The values of T_p, x_p, E, K_0, n, K_p and $-\Delta H$ of $Sb_{0.16}As_zSe_{0.84-z}$ alloys in non-isothermal crystallization

z	β (K min^{-1})	T_p (K)	x_p	E (kJ mol^{-1})	K_0 (s^{-1})	n	$K_p \times 10^3$ (s^{-1})	$-\Delta H$ (J g^{-1})
0.22	1	465	0.48	107 ± 3	1.0×10^9	2.3 ± 0.4	14.9 ± 1.2	33 ± 2
	2	479	0.47					34 ± 2
	4	485	0.50					36 ± 2
	8	504	0.54					38 ± 2
	16	515	0.51					38 ± 2
	32	527	0.43					37 ± 2
	64	539	0.44					39 ± 3
0.29	1	510	0.44	156 ± 6	1.3×10^{13}	2.7 ± 0.5	15.7 ± 1.1	32 ± 1
	2	516	0.47					36 ± 1
	4	525	0.49					49 ± 2
	8	535	0.44					52 ± 2
	16	545	0.45					41 ± 2
	32	557	0.49					51 ± 2
	64	570	0.53					50 ± 2
0.36	1	545	0.47	195 ± 6	8.2×10^{15}	2.2 ± 0.3	16.2 ± 1.6	28 ± 1
	2	549	0.54					32 ± 1
	4	555	0.41					22 ± 2
	8	565	0.57					30 ± 2
	16	574	0.48					30 ± 1
	32	584	0.48					35 ± 2
	64	599	0.43					31 ± 2
0.43	1	555	0.49	163 ± 5	2.1×10^{12}	2.3 ± 0.3	14.6 ± 1.3	40 ± 1
	2	566	0.50					41 ± 1
	4	575	0.50					40 ± 1
	8	593	0.55					37 ± 2
	16	600	0.51					38 ± 2
	32	609	0.49					42 ± 1
	64	625	0.48					46 ± 2

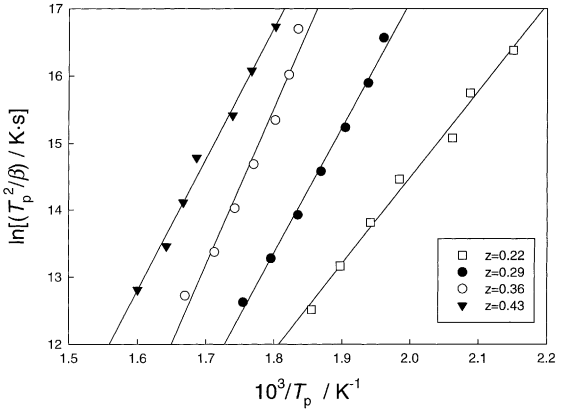

Fig. 7. Plots of $\ln(T_p^2/b)$ vs. $1/T_p$ and regression lines for the studied alloys.

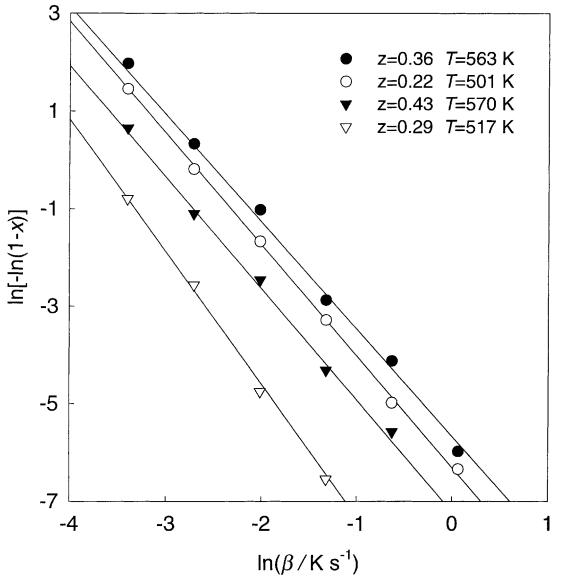

Fig. 8. $\ln[-\ln(1-x)]$ vs. $\ln\beta$ curves of the different alloys.

crystallization exotherm also increases. The crystallization of amorphous state consists of two individual processes: nucleation and crystal growth. For glasses to nucleate, a certain period of incubation is necessary. With the increase of heating rate, the time which is needed to reach a desired temperature would be reduced, thus crystallization initiates at a relatively higher temperatures, T_p correspondingly shifts to higher temperature. Generally, glasses undergo structure relaxation [19] through which glasses transform from an unstable state to a stable one before the occurrence of devitrification. The time for this transformation is shortened by the increasing of heating rate, causing the energy of structure relaxation not to be released. This part of unreleased energy is contained in the crystallization enthalpy which is determined by the area of DSC exotherm. The peak temperature, T_p, the volume fraction transformed, x_p, at T_p, and $-\Delta H$ are listed in Table 2. The four linear functions in Fig. 7 represent the least squares fits to the data of $\ln(T_p^2/\beta)$ and $1/T_p$ for the four tested samples. From the slope and intercept of these fits, E and K_0 are evaluated. The least squares fits of $\ln[-\ln(1-x)]$ versus $\ln\beta$ are illustrated in Fig. 8. They are straight lines from whose slope n is obtained. The kinetic results of $Sb_{0.16}As_zSe_{0.84-z}$ alloys for non-isothermal crystallization are also listed in Table 2, they are calculated through least squares fitting with all correlation factors >0.968.

Using kinetic parameters such as E to interpret the relative stability of glasses is complex and uncertained in some cases. In this work, the method proposed by Hu and Jiang [20] is adopted. By means of the quoted method, the parameter K_p is calculated to evaluate the thermal stability by considering the effect of both E and K_0:

$$K_p = K_0 \exp\left(-\frac{E}{RT_p}\right), \tag{18}$$

where reaction rate constant at T_p is used to compare the stability of different glass compositions. The values of E and K_0 under the heating rate of 16 K min^{-1} have been substituted into Eq. (2) to estimate K_p. The results are also listed in Table 2.

6. Identification of the crystalline phases

Taking into account the crystallization exothermal peaks shown by the glassy alloys with compositions of $z = 0.22$, 0.29, 0.36 and 0.43 it is recommended to try to identify the possible phases that crystallize after the thermal treatment applied to the samples by means of adequate XRD measurements. As an illustrating example, in Fig. 9 we show the most relevant portions of the diffractometer tracings for the as-quenched sample of composition $z = 0.22$ and for the same

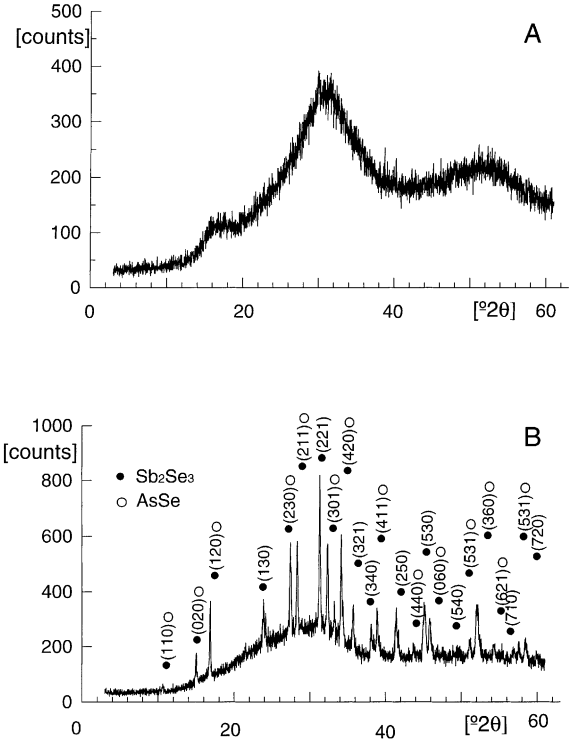

Fig. 9. (A) Diffractogram of glassy alloy $Sb_{0.16}As_{0.22}Se_{0.62}$; (B) diffraction peaks of the quoted alloy after thermal treatment.

material submitted to the thermal process. Fig. 9A has broad humps characteristic of the amorphous phase of the starting material at diffraction angles (2θ) between 20 and 60°. The diffractogram of the transformed material after the crystallization process (Fig. 9B) suggests the presence of microcrystallites of Sb_2Se_3 and AsSe indicated with (●) and (○), respectively, while there remains also a residual amorphous phase. The other compositions under study show very similar crystalline phases, after the thermal treatment. The Sb_2Se_3 phase found crystallizes in the orthorhombic system [21] with a unit cell defined by $a = 11.633$ Å, $b = 11.78$ Å and $c = 3.895$ Å.

7. Summary and conclusions

The results for both isothermal and non-isothermal crystallization kinetics of $Sb_{0.16}As_zSe_{0.84-z}$ glasses are in agreement, within experimental error, with the use of Eqs. (1) and (2), in the first regime, and with the use of Eqs. (2) and (6), in the second one, respectively, bearing in mind the corresponding assumptions clearly stated in Sections 3.1 and 3.2. In the isothermal and non-isothermal DSC studies (a) the change of crystallization time and exotherm height with time, and (b) the dependence of T_p on heating rate reveal that the crystallization of the glass is a thermally activated process, glasses undergo structure relaxation before crystallization. The crystallization energies, E, of $Sb_{0.16}As_zSe_{0.84-z}$ samples are mainly between 100 and 200 kJ mol^{-1}. It is possible to assume that, like other glass forming system [22], the crystallization may be diffusion-controlled. Further, the kinetic exponent, n, is directly determined by the mechanism of crystallization. Mahadevan et al. [23] have pointed out that n may be 4, 3, 2 or 1, which are related to different crystallization mechanism: $n = 4$, volume nucleation, three-dimensional growth; $n = 3$, volume nucleation, two-dimensional growth; $n = 2$, volume nucleation, one-dimensional growth; $n = 1$, surface nucleation, one-dimensional growth from surface to the inside. Given that the calculated values of kinetic exponent are between 2 and 3, it is possible to assume that the glass–crystal transformation of all studied alloys occurs by a mechanism of volume nucleation with one- and two-dimensional growth. Further, the kinetic data reveal the differences in glass stability among the analyzed compositions. From the *T–T–T* graph in isothermal crystallization, for example, it is obvious that the $(T_{iso} - T_g)$ versus t plot of $z = 0.43$ sample lies above, while the plot of $z = 0.36$ sample lies below the others. This difference demonstrates that in the same $(T_{iso} - T_g)$ range, $z = 0.43$ sample, which requires the longest time to be fully crystallized, has the greatest stability against devitrification, while $z = 0.36$ glass which can be crystallized easily is the least stable composition. Finally, from the non-isothermal treatment is obtained that the K_p of $z = 0.43$ sample is the smallest, reflecting its slow rate of crystallization at T_p. This results is consistent with that obtained from the *T–T–T* graph corresponding to isothermal processes.

Acknowledgements

The authors are grateful to the Junta de Andalucía and the CICYT (Comisión Interministerial de Ciencia

y Tecnología, Project number MAT98-0791) for their financial support.

References

[1] H.E. Kissinger, J. Res. NBS 57 (1957) 217.
[2] H.E. Kissinger, Anal. Chem. 29 (1957) 1702.
[3] K.H.J. Bushow, N.M. Beekmans, Physica Status Solidi (a) 60 (1980) 193.
[4] J.W. Graydon, S.J. Thorpe, D.W. Kirk, Acta Metall. Mater. 42 (1994) 3163.
[5] J. Vázquez, C. Wagner, P. Villares, R. Jiménez-Garay, J. Non-Cryst. Solids 235/237 (1998) 548.
[6] P.L. López-Alemany, J. Vázquez, P. Villares, R. Jiménez-Garay, J. Alloys Comp. 285 (1999) 185.
[7] W.W. Wendlant, Thermal Methods of Analysis, 2nd Edition, Wiley, New York, 1974.
[8] D.W. Henderson, J. Non-Cryst. Solids 30 (1979) 301.
[9] M. Avrami, J. Chem. Phys. 7 (1939) 1103.
[10] M. Avrami, J. Chem. Phys. 8 (1940) 212.
[11] M. Avrami, J. Chem. Phys. 9 (1941) 177.
[12] H. Yinnnon, D.R. Uhlmann, J. Non-Cryst. Solids 54 (1983) 253.
[13] V. Erukhimovitch, J. Baram, J. Non-Cryst. Solids 208 (1996) 288.
[14] M. Abramowitz, I.E. Stegun, Handbook of Mathematical Functions, Dover, New York, 1972.
[15] I.S. Gradshteyn, I.M. Ryzhik, Table of Integrals, Series and Products, Academic Press, New York, 1980.
[16] C.D. Doyle, Nature 207 (1965) 290.
[17] J. Vázquez, C. Wagner, P. Villares, R. Jiménez-Garay, Acta Mater. 44 (1996) 4807.
[18] K. Matusita, T. Komatsu, R. Yokota, J. Mater. Sci. 19 (1984) 291.
[19] J. Liang, Z. Chai, S. Zhao, Sci. Chin. A (1990) 105.
[20] L. Hu, Z. Jiang, J. Chin. Ceram. Soc. 18 (1990) 315.
[21] S.A. Dembovski, Russ. J. Inorg. Chem. 8 (1963) 798 (English translation).
[22] R.S. Tiwari, J. Non-Cryst. Solids 83 (1986) 126.
[23] S. Mahadevan, A. Giridar, A.K. Singh, J. Non-Cryst. Solids 88 (1986) 11.